

Spin density functional study on magnetism of potassium loaded Zeolite A

Yoshiro Nohara¹, Kazuma Nakamura², and Ryotaro Arita²

¹Department of Physics, University of Tokyo, Tokyo 113-0022, Japan and

²Department of Applied Physics, University of Tokyo, Tokyo 113-8656, Japan

(Dated: August 9, 2018)

In order to clarify the mechanism of spin polarization in potassium-loaded zeolite A, we perform *ab initio* density-functional calculations. We find that (i) the system comprising only non-magnetic elements (Al, Si, O and K) can indeed exhibit ferromagnetism, (ii) while the host cage makes a confining quantum-well potential in which *s*- and *p*-like states are formed, the potassium-4*s* electrons accommodated in the *p*-states are responsible for the spin polarization, and (iii) the size of the magnetic moment sensitively depends on the atomic configuration of the potassium atoms. We show that the spin polarization can be described systematically in terms of the confining potential and the crystal field splitting of the *p*-states.

PACS numbers: 73.22.-f, 75.75.+a, 82.75.Vx

Searching for novel ferromagnets comprising only non-magnetic elements has been a fascinating challenge in condensed matter physics. Up to present, motivated by fundamental interests or potential technological importance, various ferromagnets with non-magnetic elements have been synthesized.^{1,2} Among them, the alkali-metal-loaded zeolite is certainly a unique ferromagnet. Depending on the crystal structure of the host cage and the number/species of the guest cluster atoms, it exhibits not only ferromagnetism but also a rich variety of magnetic properties.^{3,4} In fact, one can envisage to design and control the magnetic properties of this system by choosing appropriate combinations of the guests and hosts.⁵

When we consider such materials design, the first step we should take is to clarify the mechanism of the spin polarization in this system. Indeed, it is of great interest to consider why clusters of alkali atoms confined in zeolite cages can be magnetic, even though the bulk alkali metals are usually non-magnetic. However, while almost 20 years have passed since the seminal discovery of the spin-polarized ground state in zeolite A,³ *ab initio* studies on magnetism in zeolitic materials have been quite limited so far. This is mainly because (i) the electronic structure is expected to be very complicated since the unitcell of the system is extremely huge [typically it has $O(100)$ atoms and the lattice constant is ~ 30 Å], and (ii) the atomic configuration has not been determined accurately in experiments due to the extreme complexity in the structure of the system.

However, fortunately, the situation of potassium-loaded zeolite A ($K_{12+n}Si_{12}Al_{12}O_{48}$, hereafter we call it as K-LTA) is different; a detailed neutron powder diffraction study has been performed⁶ and thus we exceptionally have a reliable reference for *ab initio* calculations. On top of that, recent density functional calculations based on local density approximation (LDA) have clarified that the low-energy electronic structure of this compound is quite simple.⁵ Namely, the system is regarded as a *super-crystal*, where guest potassium clusters act as a *superatom* with well-defined *s*- and *p*-like orbitals.⁷ Thus, we may expect that the low energy physics is expected

to be described systematically in terms of a superatom.

Experimentally, the spin polarization in K-LTA is observed when we introduce more than two potassium atoms (i.e., $n > 2$) and the Curie and Weiss temperature take their maximum at $n \sim 4$. If we follow the picture mentioned above, the superatom *s* state is fully occupied and three *p* states are partially filled for $n \sim 4$. While several scenarios for the spin polarization in K-LTA based on the assumption that the orbital degeneracy of the *p* states plays a crucial role have been proposed,^{8,9,10} an *ab initio* calculation based on spin density functional theory has yet to be done. The purpose of the present study is to clarify the mechanism of spin polarization in K-LTA from first principles. We examine in detail (i) whether a ferromagnetic ground state is really realized just from Si, Al, O and K, and (ii) if it does, for which condition the system has spin polarization. Hereafter, we focus on the case of $n = 4$, where the energy scale of magnetism is expected to be highest.

Let us see the detail of the atomic configuration considered in the present study. Figure 1 shows the atomic geometry determined by the neutron measurement with an assumption that the system has the symmetry of space group F23.⁶ Due to the Lowenstein rule (Si and Al should be arranged alternately), the unitcell contains two large (small) alminosilicate cages which we call α (β) cages (upper left panel). While a simplified unitcell having one α and β cage (which violates the Lowenstein rule) is employed in the previous LDA calculation,⁵ here we adopt the original unitcell having ~ 200 atoms. Hereafter, we label the two α cages as α_1 and α_2 (upper right panel). While the positions of Al, Si, and O were uniquely determined by the measurement, the experiment found several possible positions for potassium atoms in the α cages (bottom panel). Following this observation, we denote the center of six-, four-, and eight-membered rings in the α cage as site I, II, and III, respectively. The site IV is the center of the α cage. In order to indicate which α cage the site I, III, and IV belong to, we label them with subscript such as site I_{α_1} or I_{α_2} . Notice that the site II is on the border of two α cages.

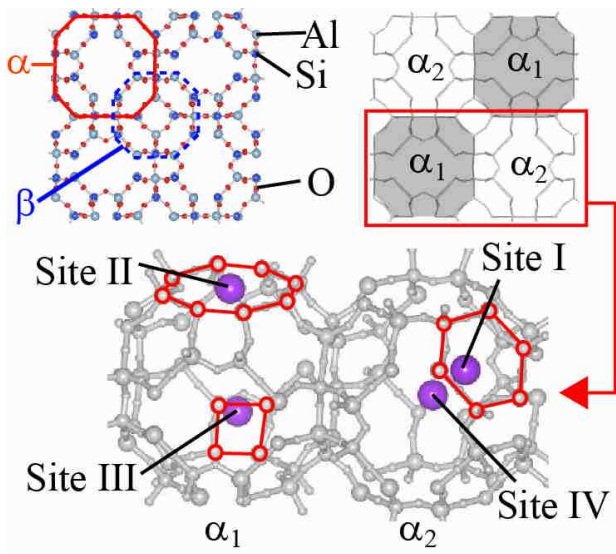


FIG. 1: (Color online) Upper left: Overall profile of zeolite LTA, where O, Al, Si atoms are denoted by red-small, light-blue, and dark-blue spheres, respectively. α and β cages are marked by red-solid and blue-dashed lines, respectively. Upper right: Two kinds of α cages (α_1 and α_2). Lower panel: Four kinds of sites occupied by potassiums (purple-large spheres). For the definition of the sites I-IV, see the text.

The experimental occupation numbers of site I_{α_1} , I_{α_2} , II, III_{α_1} , III_{α_2} , IV_{α_1} , and IV_{α_2} are 8.0, 8.0, 6.4, 5.9, 3.5, 0.0, and 0.5, respectively. In the present calculation, for simplicity, we assume the occupation numbers as 8, 8, 6, 6, 3, 0, and 1. Thus the site I, II and IV_{α_2} are fully occupied and the site IV_{α_1} is completely vacant.¹¹ Note that the total number of the potassium atoms is 32, and the number of site I, II, III in the unitcell is 16, 6 and 24, respectively. While the atomic configuration of the site I, II and IV are uniquely determined, there are huge possibilities for the configuration of the site III; since there are 24 possible positions and we have nine potassium atoms in the site III (6 for the α_1 cage and 3 for the α_2 cage), we have ${}_{12}C_6 \times {}_{12}C_3 = 203280$ possibilities.

Thus in the present study, we focus on the following four geometries I-IV with trigonal symmetry shown in Fig. 2. In those geometries, we have two triangles and a hexagon in the α_1 cage, and a small triangle and a large triangle in the α_2 cage. We note that, for the geometries I and III, the site-III and site-IV potassiums in the α_2 cage make a tetrahedron.

Ab initio calculations based on local spin density approximation (LSDA) were performed with *Tokyo Ab initio Program Package*.¹² We used the GGA exchange-correlation functional,¹³ plane-wave basis set, and the ultrasoft pseudopotentials¹⁴ in the Kleinman-Bylander representation.¹⁵ The pseudopotential of potassium was supplemented by the partial core correction.¹⁶ The energy cutoff of plane waves representing wavefunctions is

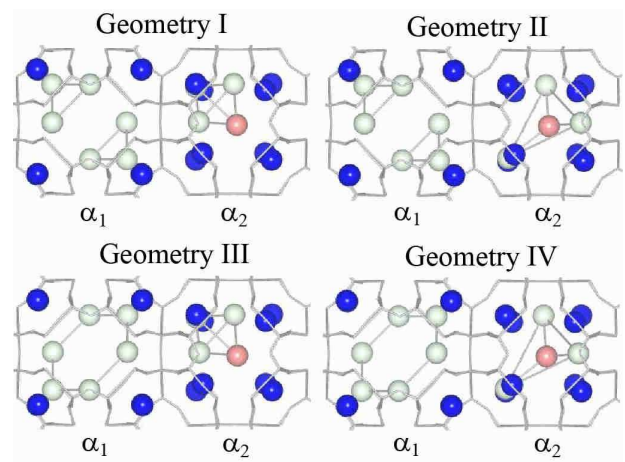


FIG. 2: (Color online) Four geometries considered in the present study, where dark-blue, light-green, and medium-red spheres stand for the potassiums occupying the site I, III, and IV, respectively. The difference in each geometry comes from the difference in the configuration of site-III potassiums; “two triangles” and “small triangle” (geometry I), “two triangles” and “large triangle” (geometry II), “hexagon” and “small triangle” (geometry III), and “hexagon” and “large triangle” (geometry IV) are accommodated in the α_1 and α_2 cages. We note that four site-I potassiums in the α_1 cage are overlapped with the remaining four site-I potassiums in this view.

36 Ry and a $4 \times 4 \times 4$ k -point sampling is employed.

We show in TABLE I the total energies calculated for the geometries I-IV, together with local magnetic moments in each α cage.¹⁷ We see that the site-III configuration significantly affects the energetics and the value of the magnetic moment. Interestingly, for all the geometries, the moment develops in the α_2 cage, which suggests that the valence electrons responsible for the magnetism reside mainly in the α_2 cage. This is because the confining potential of the α_2 cage is deeper than that of α_1 ; as seen from Fig. 2, the site-I potassiums in the α_2 cage exist at inner side than those in the α_1 cage, which makes the electrostatic potential in the α_2 cage deeper.

TABLE I: Total energy per unitcell of each geometry ΔE_{tot} with reference to that of the geometry I and the local magnetic moments M_i in the α_i cage ($i = 1$ or 2) (Ref. 17). For the definition for the geometries I-IV, see Fig. 2.

	Geom I	Geom II	Geom III	Geom IV
$\Delta E_{\text{tot}}(\text{eV})$	0	1.02	1.49	0.12
$M_1(\mu_B)$	-0.02	-0.20	0.06	-0.16
$M_2(\mu_B)$	1.92	0.33	1.36	1.00

Another important point in TABLE I is that the size of the magnetic moment depends on the atomic configuration of the potassium cluster. In order to clarify its

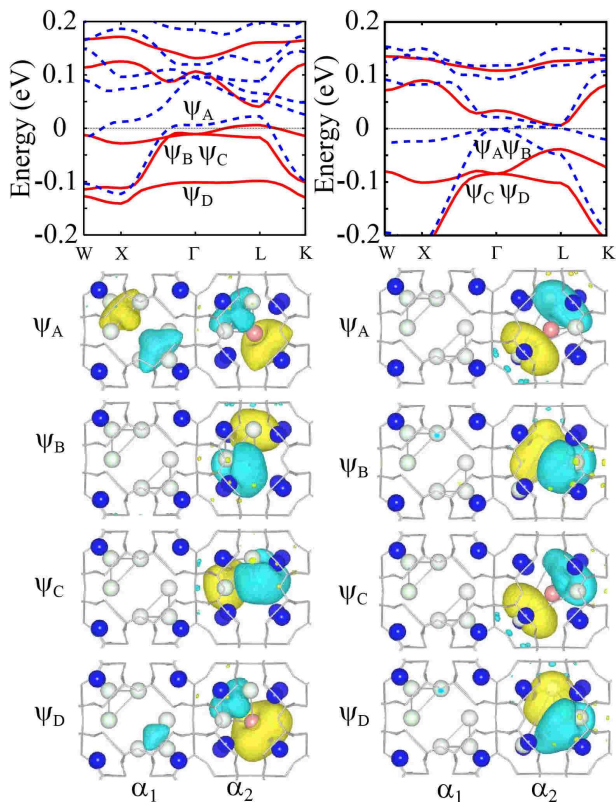


FIG. 3: (Color online) Calculated GGA band dispersions (upper) and Bloch wavefunctions, Ψ_A - Ψ_D , at the Γ point (lower) for the geometries I (left) and II (right). In the band dispersion, red-solid and blue-dashed lines stand for majority and minority spin states, respectively. The energy zero is set to the Fermi level. In the wavefunctions, isosurfaces are drawn by the values of ± 0.015 (a.u.). Potassiums occupying the site I, III, and IV are displayed by spheres of the same colors with Fig. 2.

origin, we calculated the low-energy bands and their wavefunctions. In the upper left (right) panel in Fig. 3, we show the low-energy band structures near the Fermi level for the geometries I (II), corresponding to the second (third) column in TABLE I. While the band structure is quite different for these two geometries, the Bloch wavefunctions at the Γ point (Ψ_A - Ψ_D) have common features; (i) they have large amplitude in the α_2 cage due to the deeper cage potential in α_2 mentioned above, and (ii) they widely spread in the α cage without localizing on any specific atoms and are regarded as *superatom* p -type wavefunctions.⁵

To make the situation clearer, in Fig. 4, we draw level diagrams of the low-energy states where the cage potentials, superatom p levels, and spin configurations are depicted schematically. Here, the p states are represented in the local coordinates, where the z axis is taken to be perpendicular to the triangles in α cages (see Fig. 2). In the geometry I (upper left), for both the α cages, the superatom p_x and p_y levels are degenerated and higher

than the p_z level. This can be understood as follows: In the α_1 cage, the superatom p_z lobe extends in the direction of the center of the triangle and feels a positive crystal field, lowering the level of p_z . The same mechanism works in the α_2 cage, and the low-lying p_z states in α_1 and α_2 cages form a σ bonding orbital. On the other hand, the p_x and p_y states in the α_2 cage, with a non-bonding character, reside near the Fermi level. In the present case of $n = 4$, there are four superatom p electrons. Two electrons accommodated in the σ bonding orbital and the remaining two electrons occupy the degenerated p_x and p_y orbitals. According to the Hund's rule, electron spins in the degenerated orbitals align to be parallel, thus generate the magnetic moment of $\sim 2 \mu_B$.

For the geometry II (upper right panel in Fig. 4), in the α_2 cage, the level of p_z is higher than p_x and p_y . This can be also understood in terms of the crystal field formed by the site-III potassiums in the α_2 cage. In this configuration, the p_x and p_y orbitals lie in the “large” triangle plane and thus these states are stabilized electrostatically, compared to the p_z state. Consequently, in the geometry II, the four electrons fully occupy the p_x and p_y states, so that the system has smaller magnetic moments.

A similar argument can hold also in the cases of the geometries III and IV. In these geometries, the α_1 cage contains a hexagon instead of two triangles. The crystal field in the α_1 cage stabilizes the p_x and p_y states in the hexagon plane. In the geometry III (lower left panel in Fig. 4), the two electrons occupy the low-lying p_z orbital

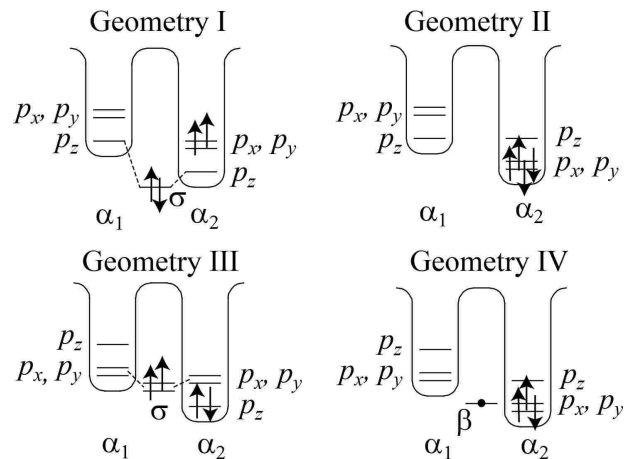


FIG. 4: Level diagrams for electronic structures of the four geometries displayed in Fig. 2, where superatom p levels in the α_1 - and α_2 -cage potentials and the resulting spin configurations are drawn schematically. The p states are represented in the local coordinates (for the definition, see the text). The difference between the cage potentials of α_1 and α_2 comes from the difference in the configuration of the site-I potassiums (see Fig. 2) and the p -level splitting is due to the site-III-potassium configurations.

in the α_2 cage and the degenerated σ orbitals made from the p_x and p_y states in the α_1 and α_2 cages accommodate the remaining two electrons. Because the σ orbital is less localized, the value of the moment is somewhat reduced ($\sim 1.5 \mu_B$), compared to that of the geometry I. In the geometry IV (lower left panel), an extra state in the β cage appears near the Fermi level. This state has a large dispersion and small spin polarization. The net moment is generated from the three electrons occupying the degenerated p_x and p_y orbitals, with the value of the moment $\sim 1 \mu_B$.

Thus, we conclude that K-LTA can be ferromagnetic in LSDA and the mechanism of the spin polarization is consistently explained in view of the superatom picture; if the p levels formed by the superatom wavefunctions are degenerated and partially occupied, the system becomes magnetic, due to the Hund's rule coupling in these states. This condition and the size of the moment are controlled by the atomic configuration of the guest potassium clusters, responsible for the cage-potential depth and the crystal field inducing the p -level shift and split, respectively.

Experimentally, two kinds of possible magnetic structures have been proposed for K-LTA. One is the ferromagnetic model,¹⁰ and the other is the spin-canted antiferromagnetic model.⁹ In the former, the system consists of two sublattices with large ($\sim 2.8 \mu_B$) and small (almost $0.0 \mu_B$) magnetic moment, while, in the latter, every α cage has a moment of $1 \mu_B$. These magnetic structures look like the results for the geometries I and IV, although the size of the moments is relatively smaller than the experimental values. It is interesting to note that the geometries I and IV have comparable energies

(see TABLE I).

In reality, the site III is randomly occupied.⁶ It is formidable or almost impossible to take into account the randomness of the site III explicitly in the first-principles calculation. However, the superatom picture has been shown to capture essential features of the low energy physics of K-LTA. Thus, a multi-orbital Hubbard-type model with random potentials would be served as a realistic low-energy model describing magnetism of the system. Since all the parameters characterizing the Hubbard model can be derived with first-principle basis as was recently done in Ref. 18, we can discuss the magnetism in more realistic situations by solving this effective model. It will be an important future study.

To summarize, by means of *ab initio* spin density functional calculation, we found that (i) K-LTA comprising only Al, Si, O and K can be ferromagnetic, (ii) the superatom p states are responsible for the magnetism, and (iii) the magnetic property of K-LTA depends sensitively on the atomic configuration of the guest potassium cluster. The condition for the spin polarization was presented and understood systematically in terms of the superatom picture. Our findings provide a firm basis and will be the first step for clarifying the low-energy physics in zeolitic materials.

We thank Professor Yasuo Nozue, Takehito Nakano, and Mutsuo Igarashi for fruitful discussions. This work was supported by Scientific Research on Priority Areas of New Materials Science Using Regulated Nano Spaces (No. 19051016) MEXT, Japan. All the computations have been performed on Hitachi SR11000 system at the Supercomputing Division, Information Technology Center, the University of Tokyo.

-
- ¹ P.-M. Allemand, K. C. Khemani, A. Koch, F. Wudl, K. Holczer, S. Donovan, G. Grüner, and J. D. Thompson, *Science* **253**, 301 (1991).
- ² M. Takahashi, P. Turek, Y. Nakazawa, M. Tamura, K. Nozawa, D. Shiomi, M. Ishikawa, and M. Kinoshita, *Phys. Rev. Lett.* **67**, 746 (1991).
- ³ Y. Nozue, T. Kodaira, and T. Goto, *Phys. Rev. Lett.* **68**, 3789 (1992); Y. Nozue, T. Kodaira, S. Ohwashi, T. Goto, and O. Terasaki, *Phys. Rev. B* **48**, 12253 (1993).
- ⁴ V. I. Srdanov, G. D. Stucky, E. Lippmaa, and G. Engelhardt, *Phys. Rev. Lett.* **80**, 2449 (1998). T. Nakano, K. Goto, I. Watanabe, F. L. Pratt, Y. Ikemoto, and Y. Nozue, *Physica B* **374-375**, 21 (2006).
- ⁵ R. Arita, T. Miyake, T. Kotani, M. van Schilfgaarde, T. Oka, K. Kuroki, Y. Nozue, and H. Aoki, *Phys. Rev. B* **69**, 195106 (2004).
- ⁶ T. Ikeda, T. Kodaira, F. Izumi, T. Kamiyama, and K. Ohshima, *Chem. Phys. Lett.* **318**, 93 (2000).
- ⁷ W. D. Knight, K. Clemenger, W. A. de Heer, W. A. Saunders, M. Y. Chou, and M. L. Cohen, *Phys. Rev. Lett.* **52**, 2141 (1984); W. Ekardt, *Phys. Rev. B* **29**, 1558 (1984).
- ⁸ T. Nakano, and Y. Nozue, *J. Comp. Meth. Sci. Eng.* **7**, 443 (2007); T. Nakano, Doctor Thesis, (2000).
- ⁹ T. Nakano, D. Kiniwa, Y. Ikemoto, and Y. Nozue, *J. Magn. Mater.* **272-276**, 114 (2004).
- ¹⁰ H. Kira, H. Tou, Y. Maniwa, and Y. Murakami, *Physica B* **312-313**, 789 (2002).
- ¹¹ In the experiment, the exact position of a half of the site-I potassiums is slightly different from the center of the six-membered ring and two positions for the site I have been observed. The occupancies are different (57 % and 43 %). In the present study, we employ the high-probability position for all the site-I potassiums.
- ¹² J. Yamauchi, M. Tsukada, S. Watanabe, and O. Sugino, *Phys. Rev. B* **54**, 5586 (1996).
- ¹³ J. P. Perdew, K. Burke, and M. Ernzerhof, *Phys. Rev. Lett.* **77**, 3865 (1996).
- ¹⁴ D. Vanderbilt, *Phys. Rev. B* **41**, 7892 (1990).
- ¹⁵ L. Kleinman, and D. M. Bylander, *Phys. Rev. Lett.* **48**, 1425 (1982).
- ¹⁶ S. G. Louie, S. Froyen, and M. L. Cohen, *Phys. Rev. B* **26**, 1738 (1982).
- ¹⁷ The local magnetic moment of α cages was calculated for the Voronoi polyhedron having the same volume as that of the sphere of the radius of 7.64 Å.
- ¹⁸ K. Nakamura, T. Koretsune, R. Arita, arXiv:0907.4593.